

Bell-inequality violations with single photons entangled in momentum and polarization

B R Gadway^{1,3}, E J Galvez¹ and F De Zela²

¹ Department of Physics and Astronomy, Colgate University, Hamilton, NY 13346, USA

² Departamento de Ciencias, Sección Física, Pontificia Universidad Católica del Perú, Apartado 1761, Lima, Peru

E-mail: egalvez@mail.colgate.edu

Received 15 July 2008, in final form 17 November 2008

Published 16 December 2008

Online at stacks.iop.org/JPhysB/42/015503

Abstract

We present a violation of the Clauser–Horne–Shimony–Holt and the Clauser–Horne inequalities using heralded single photons entangled in momentum and polarization modes. A Mach–Zehnder interferometer and polarization optics are used to rotate the spatial and polarization bases, respectively. With this setup we were able to test quantum mechanics with the original formulation of the Clauser–Horne inequality. The results rule out a wide class of realistic non-contextual hidden-variable theories.

(Some figures in this article are in colour only in the electronic version)

1. Introduction

One of the great quests in physics today is to prove via experiments the fundamental tenets of quantum mechanics: that nature is not realistic (i.e. observables do not have pre-existing values), that it is indeterministic (i.e., that the results of future measurements are not determined by initial conditions), contextual (i.e., that measurement outcomes can depend on the context, e.g., on measurement outcomes for comeasurable observables) and nonlocal (i.e., that measurement outcomes at two spacelike separated locations can be correlated with one another more strongly than allowed classically). These are pursued either alone or combined. Ever since the famous discussions of Bohr and Einstein at the Solvay meetings of the early twentieth century (Wheeler and Zurek 1983), and the classic Einstein–Podolski–Rosen paper (Einstein *et al* 1935), these questions have preoccupied physicists, philosophers and scientists alike. This has been enhanced by the staggering success of the soon-to-be 100-year-old theory of quantum mechanics in explaining natural phenomena. Some are bothered, as Einstein was, that despite living our daily lives in an apparent classical, realistic, deterministic, non-contextual and local world, we find that quantum mechanics, the theory

with the perfect record, says otherwise. The question thus arises as to whether the quantum-mechanical description of physical phenomena is the ultimate one, or whether it could be somehow completed in accordance with a realistic view of the world. Since the 1960s Bell (1965, 1966) and others (Kochen and Specker 1967, Clauser *et al* 1969, Clauser and Horne 1974) have told us that we can decide these questions in the laboratory, and technological advances have indeed allowed us to get near conclusive answers to these fundamental questions about nature and about whether quantum mechanics is truly complete or not.

The answers provided by laboratory experiments are not yet conclusive because most of the tests that were designed—or performed—suffer from some ‘loopholes’. However, a number of questions have already been answered. For example, Aspect and co-workers showed via experiments with entangled photons and electro-optical devices that nature is not realistic or non-local (modulo loopholes), as maintained by quantum mechanics (Aspect *et al* 1982). More recent tests confirm these results via violations of Bell inequalities to many standard deviations and in closing some experimental loopholes (Weihs *et al* 1998, Tittel *et al* 1998, Rowe *et al* 2001). Thus the question that nature is not realistic and nonlocal appears to have been settled, although some still argue otherwise (Santos 2004).

³ Present address: Department of Physics and Astronomy, University at Stony Brook, Stony Brook, NY 11794-3800, USA.

Despite these results, it is a misconception to think that all is said and done. Hidden-variable theories that are realistic but non-local could still negate quantum mechanics. A recent experimental test has started the task of addressing this question (Groblacher *et al* 2007), but the jury is out about how conclusively (Aspect 2007).

There are also other tests that probe realism, contextuality and determinism without addressing locality. This class of measurements does not require correlated pairs of particles, but does require two qubits. Two particles are *not* needed to decide these types of tests. The two qubits can be realized by entangling two modes of the same particle. In the case of photons it can be polarization, propagation direction (Michler *et al* 2000, this work), or orbital angular momentum (Mair *et al* 2001, Barreiro *et al* 2005). In the case of massive particles (e.g., neutrons) it is momentum and spin (Hasegawa *et al* 2003). While the latter tests have ruled out non-contextual HV theories via conventional Bell-type inequalities, more recent tests with single photons (Huang *et al* 2003) have started to probe different forms of contextuality addressed by the Kochen–Specker theorem (Kochen and Specker 1967). A third class of tests, only proposed thus far, involves a single particle and a single qubit. These types of tests probe realism, contextuality, determinism, invasiveness of measurements and macro-realism (Leggett and Garg 1985, Malley 1998, Lapiedra 2006, De Zela 2007).

Another class of tests involving three or more qubits relieves the requirement of performing statistical measurements (Greenberger *et al* 1989). Such all-or-nothing tests also rule out different aspects of HV theories (Bouwmeester *et al* 1999, Michler *et al* 2000).

It is important to note that the non-contextual HV theories tested by single photons admit an important tenet of modern physics: that light at a fundamental level is quantized in the form of photons. Experimental tests of these theories use non-classical sources of light or measurements, and thus cannot be fully explained by classical wave theories. That the results of the measured intensities in these experiments are mimicked by the predictions of classical wave optics is a common source of confusion because the aim of the experiments is to test quantum mechanics, not the wave description of light. Similar tests on massive particles do not lead to the same confusion because they do not have a classical wave counterpart like light does.

Our experiments use two qubits that are carried by a single photon. They aim at testing quantum mechanics via two Bell-type inequalities, namely the Clauser–Horne–Shimony–Holt (Clauser *et al* 1969, hereafter referred to as CHSH) and the Clauser–Horne (1974, hereafter referred to as CH) inequalities. The novelty with the CHSH test introduced here is that we perform it in a form that is simpler than in a previous experiment of this type (Michler *et al* 2000). Perhaps more importantly, we perform a first test of the CH inequality with single particles. In its original form this inequality relies on a combination of single and joint probabilities. Experiments with two particles cannot reliably introduce the single-particle probabilities due to a lack of knowledge of the detection efficiencies (Clauser and Shimony 1978). We present an

analysis of the CH inequality and show that two-qubit systems can be used to perform tests of the original CH inequality because single probabilities reduce to combinations of joint probabilities with the same detection efficiency. Thus, the detection efficiencies drop out of the inequality altogether. By avoiding normalizing detector counts we avoid loopholes that may be invoked to validate HV theories.

The latter is an important point because of all reported tests of the CHSH and the CH inequalities only one does not suffer from the so-called detection loophole (Rowe *et al* 2001). In order to take into account detectors' efficiencies η without invoking auxiliary assumptions about undetected events, one has to modify the original CHSH and CH inequalities (Clauser and Horne 1974, Garg and Mermin 1987, Eberhard 1993). Quantum mechanics predicts the violation of these modified inequalities for $\eta > \eta_0$, where η_0 depends on the kind of test (two-photon, atom–photon, etc). Well-known values of η_0 are 0.83 (Garg and Mermin 1987), 0.67 (Eberhard 1993), and 0.5 (Cabello and Larsson 2007). In the present experiments the issue related to detector efficiencies drops because the inequality is independent of them.

As mentioned earlier, our tests are conducted with single particles (photons). Thus, they belong to a class of tests that was initiated by Tan *et al* (1991). There is an ongoing discussion as to whether a single-photon state can display nonlocal features or not (Tan *et al* 1991, Peres 1995, Hardy 1994, Greenberger *et al* 1995, van Enk 2005). Indeed, it has been claimed (see, e.g., Hardy (1994) and van Enk (2005)) that single-photon states like $|0\rangle_A|1\rangle_B + |1\rangle_A|0\rangle_B$ can display nonlocality. Here, $|0\rangle$ means the state with zero photons, while A and B denote two spatially separated modes. We should stress, however, that in our case the issue of nonlocality does not arise at all because in our experiments the outcome of the measurements is recorded with a single detector. That is, the system is never projected onto a superposition of different photon-number states.

This paper is organized in the following way. In section 2, we describe a general method and the corresponding theoretical framework for making experiments with single photons and two qubits. In section 3 we describe the apparatus and in section 3 we present the results of the experimental tests. Further discussions and concluding remarks are given in section 4.

2. Theoretical framework

A single photon can be prepared in an entangled state of momentum (spatial) and polarization modes of light (Englert *et al* 1999). Once the state is prepared then it can be projected into rotated bases of each mode, and thus can be used to test quantum mechanics. The production and measurement of this type of entanglement was previously adapted to an experiment for the purpose of testing non-contextual HV theories (Michler *et al* 2000). In this work we follow similar aims but apply different methods. In particular, we introduce the use of the Mach–Zehnder interferometer as a spatial-basis rotator and projector.

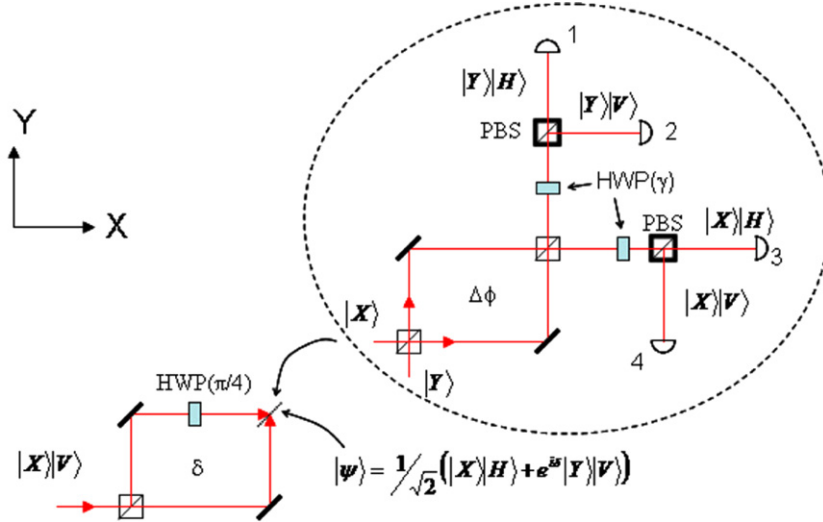


Figure 1. Schematic of the method to produce and analyse single photons entangled in the spatial and polarization modes. A state preparation arrangement (SPA) puts the light in an entangled state of polarization and momentum. The spatial basis was rotated by an angle α with a Mach-Zehnder interferometer (MZI) with a phase difference between the two paths of $\Delta\phi = 2\alpha$. The polarization basis states are rotated by an angle β using a half wave plate forming an angle $\gamma = \beta/2$. The polarization states are rotated by half-wave plates (HWP(angle)) and projected using polarization beam splitters (PBS).

We will start the discussion of our experiments by considering the use of a general setup shown schematically in figure 1. Photons are initially produced in the state $|X\rangle|V\rangle$, which represents the light propagating along the X -direction and polarized vertically (the apparatus is contained in the horizontal plane). The two-way path followed by the photon and its polarization constitute the two qubits that we employ. The standard basis of the corresponding four-dimensional Hilbert space is given by $\{|Y\rangle|V\rangle, |Y\rangle|H\rangle, |X\rangle|V\rangle, |X\rangle|H\rangle\} \equiv \{|YV\rangle, |YH\rangle, |XV\rangle, |XH\rangle\}$. This basis can be realized by any two qubits and is generally denoted as $\{|\uparrow\uparrow\rangle, |\uparrow\downarrow\rangle, |\downarrow\uparrow\rangle, |\downarrow\downarrow\rangle\}$. For our purposes, it is immaterial whether each qubit is attached to a different particle, or whether the two of them are attached to one and the same particle. In the present case, a single particle (photon) will carry both qubits.

One standard test of Bell inequalities consists of preparing the singlet-state $|\Psi^-\rangle = (|XV\rangle - |YH\rangle)/\sqrt{2}$ and submitting it to four correlation measurements (each party chooses between two local settings). When this state is realized with two particles, the two measurements take place in two distant regions. Each of these measurements amounts to a projection of a qubit along some direction, given by a unit 3-vector \vec{a} . The corresponding projector in the two-dimensional Hilbert space of the qubit being measured has the form $(I + \vec{a} \cdot \vec{\sigma})/2$, where I is the identity operator and $\vec{\sigma}$ denotes the triple of Pauli matrices. The result of each measurement can be $+1$ ('spin up') or -1 ('spin down'). Considering the projectors, $\pi_a^\pm = (I \pm \vec{a} \cdot \vec{\sigma})/2$, and $\pi_b^\pm = (I \pm \vec{b} \cdot \vec{\sigma})/2$, one can easily calculate the quantum-mechanical prediction for the probabilities of the four possible results of the measurements as

$$P(++|a, b) = \langle \Psi^- | \pi_a^+ \pi_b^+ | \Psi^- \rangle = \frac{1}{2} \sin^2 \theta_{ab}, \quad (1)$$

$$P(+ - |a, b) = \langle \Psi^- | \pi_a^+ \pi_b^- | \Psi^- \rangle = \frac{1}{2} \cos^2 \theta_{ab}, \quad (2)$$

$$P(- + |a, b) = \langle \Psi^- | \pi_a^- \pi_b^+ | \Psi^- \rangle = \frac{1}{2} \cos^2 \theta_{ab}, \quad (3)$$

$$P(- - |a, b) = \langle \Psi^- | \pi_a^- \pi_b^- | \Psi^- \rangle = \frac{1}{2} \sin^2 \theta_{ab}, \quad (4)$$

with $\theta_{ab} = \cos^{-1}(\vec{a} \cdot \vec{b})$ being the angle between vectors \vec{a} and \vec{b} . The CHSH and CH inequalities involve four unit vectors $\vec{a}, \vec{a}', \vec{b}$ and \vec{b}' . When probabilities similar to the above ones are replaced in the CHSH or in the CH inequalities and the unit vectors are properly chosen, then quantum mechanics predicts the violation of the said inequalities.

Our experimental objective is to mount an arrangement that is capable of producing an output like that of equations (1)–(4). In the latter equations $|\Psi^-\rangle$ is one of the four Bell states conforming the Bell basis, which are given by

$$|\Psi^\pm\rangle = \frac{1}{\sqrt{2}}(|XV\rangle \pm |YH\rangle), \quad (5)$$

$$|\Phi^\pm\rangle = \frac{1}{\sqrt{2}}(|XH\rangle \pm |YV\rangle). \quad (6)$$

Any one of the Bell states could be used for our purposes. In our case, we used $|\Phi^+\rangle$. To produce it, we employed the state-preparation arrangement (SPA) of figure 1, which is a gate that converts an input state from the standard basis into a state of the Bell basis. The SPA consists of a nonpolarizing 50–50 beam splitter that provides the light with two paths and a half-wave plate in the upper path, oriented to change polarization from vertical to horizontal. In the lower path the polarization of the light remains unchanged. If the light input to the SPA is in state $|XV\rangle$, then at the place where the two beams meet again the state of the light is given by

$$|\psi\rangle = \frac{1}{\sqrt{2}}(|XH\rangle + e^{i\delta}|YV\rangle), \quad (7)$$

where δ is the phase due to a difference in path lengths. Setting $\delta = 0$ gives us state $|\Phi^+\rangle$ of equation (6).

The light in this state is then submitted to a Mach-Zehnder interferometer (MZI) followed by polarization components at its output ports (within dashed lines in figure 1). The MZI is a gate whose essential action is to rotate the first qubit (Englert

et al 1999). The action of MZI can be described as the successive application of U_{BS} (for the nonpolarizing first beam splitter) followed by U_{mirror} (for the mirrors) and $U(\varphi_1, \varphi_2)$ for the phases gained by light traveling along the upper and the lower branches of the MZI. Finally, U_{BS} acts again, so that the MZI is represented by

$$U_1 = U_{BS}U(\varphi_1, \varphi_2)U_{\text{mirror}}U_{BS}. \quad (8)$$

Thus, acting on the spatial eigenvectors $|X\rangle = (1, 0)^T$ and $|Y\rangle = (0, 1)^T$ the operator U_1 is represented by the unitary matrix

$$U_1 = e^{i(\Sigma\varphi+\pi/2)} \begin{pmatrix} \cos \alpha & \sin \alpha \\ -\sin \alpha & \cos \alpha \end{pmatrix} = e^{i(\Sigma\varphi+\pi/2)} R(\alpha), \quad (9)$$

with $\alpha = (\varphi_1 - \varphi_2)/2$ and $\Sigma\varphi = (\varphi_1 + \varphi_2)/2$.

The output ports of the MZI have half-wave plates oriented at an angle γ that rotate the polarization basis $|H\rangle = (1, 0)^T$ and $|V\rangle = (0, 1)^T$ according to $U_2 = R(\beta)$, where $\beta = -2\gamma$. The result of applying $U(\alpha, \beta) = U_1(\alpha) \otimes U_2(\beta)$ on the Bell states is given by

$$U|\Phi^\pm\rangle = e^{i\Sigma\varphi}(\sin(\alpha - \beta)|\Psi^\pm\rangle - \cos(\alpha - \beta)|\Phi^\mp\rangle), \quad (10)$$

$$U|\Psi^\pm\rangle = e^{i\Sigma\varphi}(\cos(\alpha - \beta)|\Psi^\mp\rangle + \sin(\alpha - \beta)|\Phi^\pm\rangle). \quad (11)$$

Each of the above four states can be used to violate a Bell-like inequality. Take, for example, $U|\Phi^+\rangle = e^{i\Sigma\varphi}(\sin(\alpha - \beta)|\Psi^+\rangle - \cos(\alpha - \beta)|\Phi^-\rangle)$ as the state on which our system has been prepared. The probabilities of detecting the states belonging to the standard product basis $\{|XH\rangle, |XV\rangle, |YV\rangle, |YH\rangle\}$ are then given by

$$P_{XH} = |\langle XH|U|\Phi^+\rangle|^2 = \frac{1}{2} \cos^2(\alpha - \beta), \quad (12)$$

$$P_{XV} = |\langle XV|U|\Phi^+\rangle|^2 = \frac{1}{2} \sin^2(\alpha - \beta), \quad (13)$$

$$P_{YH} = |\langle YH|U|\Phi^+\rangle|^2 = \frac{1}{2} \sin^2(\alpha - \beta), \quad (14)$$

$$P_{YV} = |\langle YV|U|\Phi^+\rangle|^2 = \frac{1}{2} \cos^2(\alpha - \beta). \quad (15)$$

The outputs of the MZI project the state in the spatial basis states, and the outputs of the polarizing beam splitters project the state further into the polarization basis states. Thus, each of the detectors records the events when the light is projected on each of the product basis states, and thus over time gives signals that are proportional to the probabilities of equations (12)–(15). It is well known that with these probabilities it becomes possible to violate Bell-type inequalities such as the CHSH and the CH inequalities.

2.1. Clauser–Horne–Shimony–Holt inequality

The CHSH inequality follows from the assumptions underlying non-contextual hidden-variable theories and, in our case, constrains the degree of spatial and polarization correlations for measurements at different rotation angles. The inequality uses the correlation parameter

$$S_{\text{CHSH}} = E(\alpha, \beta) - E(\alpha, \beta') + E(\alpha', \beta) + E(\alpha', \beta'), \quad (16)$$

where $E(\alpha, \beta)$ is given by

$$E(\alpha, \beta) = P_{XH}(\alpha, \beta) + P_{YV}(\alpha, \beta) - P_{XV}(\alpha, \beta) - P_{YH}(\alpha, \beta). \quad (17)$$

The CHSH inequality states that any non-contextual HV theory satisfies $|S| \leq 2$. For a suitable choice of angles, for example $\alpha = -\pi/4, \alpha' = -\pi/2, \beta = -3\pi/8$ and $\beta' = 3\pi/8$, quantum mechanics predicts $S_{\text{CHSH}} = 2\sqrt{2}$. This follows from $E(\alpha, \beta) = \cos(2(\alpha - \beta))$.

In the experiment, the probabilities that would enter the definition of $E(\alpha, \beta)$ are determined by four photon counts $N(\alpha, \beta)$. For example, $P_{YV}(\alpha, \beta) = N_1(\alpha, \beta)/N$. Since it is difficult to obtain a reliable measure of the detection efficiency, and therefore N , it is customary to redefine the correlation parameter S in terms of the normalized parameters E^* instead of E , where $E^* = (N_{XH} + N_{YV} - N_{XV} - N_{YH}) / (N_{XH} + N_{YV} + N_{XV} + N_{YH})$. However, such an expedient has given rise to objections on the validity of the test (Santos 2004).

2.2. Clauser–Horne inequality

In the CH inequality, any four numbers x_1, y_2, x'_1, y'_2 lying in the interval $[0, 1]$ satisfy

$$x_1 y_2 - x_1 y'_2 + x'_1 y_2 + x'_1 y'_2 - x'_1 - y_2 \leq 0. \quad (18)$$

Starting from this inequality, any non-contextual HV theory predicts

$$S_{\text{CH}} \equiv P_{YV}^{cl}(\alpha, \beta) - P_{YV}^{cl}(\alpha, \beta') + P_{YV}^{cl}(\alpha', \beta) + P_{YV}^{cl}(\alpha', \beta') - P_Y^{cl}(\alpha') - P_V^{cl}(\beta) \leq 0. \quad (19)$$

The correlations $P_{YV}^{cl}(\alpha, \beta)$ are classical probabilities for the two involved outcomes, in this case corresponding to vertically polarized photons (V) measured in the upper branch (Y) under different angles, given by α and β . These classical quantities have the forms $P_r^{cl}(\alpha) = \int d\lambda \rho(\lambda) p_r(\lambda, \alpha)$ and $P_{rs}^{cl}(\alpha, \beta) = \int d\lambda \rho(\lambda) p_r(\lambda, \alpha) p_s(\lambda, \beta)$, with r, s specifying the measurement result (X or Y , and H or V , in our case). The label λ stands for one or more hidden variables underlying a complete description of the state produced at the source with probability density $\rho(\lambda)$, whereas $p_r(\lambda, \alpha)$ is the probability of obtaining the result r when the detector was set as specified by α , the detection being performed on a particle characterized by λ . Non-contextuality has been invoked by setting $p_{rs}(\lambda, \alpha, \beta) = p_r(\lambda, \alpha) p_s(\lambda, \beta)$ and by assuming a probability density $\rho(\lambda)$ that depends only on the set λ of hidden variables, i.e., being independent of (α, β) .

If instead of using the classical correlations we use the quantum mechanical ones, as given by equations (12)–(15), we can predict a violation of the inequality (19). Indeed, observing that $P_Y(\alpha) = P_{YV}(\alpha, \beta'') + P_{YH}(\alpha, \beta'') = 1/2$, $P_V(\beta) = P_{YV}(\alpha'', \beta) + P_{XV}(\alpha'', \beta) = 1/2$ and using (19) we get

$$S_{\text{CH}} = \cos^2(\alpha - \beta) - \cos^2(\alpha - \beta') + \cos^2(\alpha' - \beta) + \cos^2(\alpha' - \beta') - 2 \leq 0. \quad (20)$$

Setting $\alpha = -\pi/4, \alpha' = -\pi/2, \beta = -3\pi/8, \beta' = 3\pi/8$, we obtain $S_{\text{CH}} = 0.207$, in contradiction with the prediction of a HV theory.

As will be explained in detail in the following section, in our experiment we detect the photons with a single detector set at the output of the SPA and MZI arrangements (see figure 2), instead of using the four detectors that appear in figure 1. In what follows, we justify why—in spite of using a single detector—we could still have a valid test.

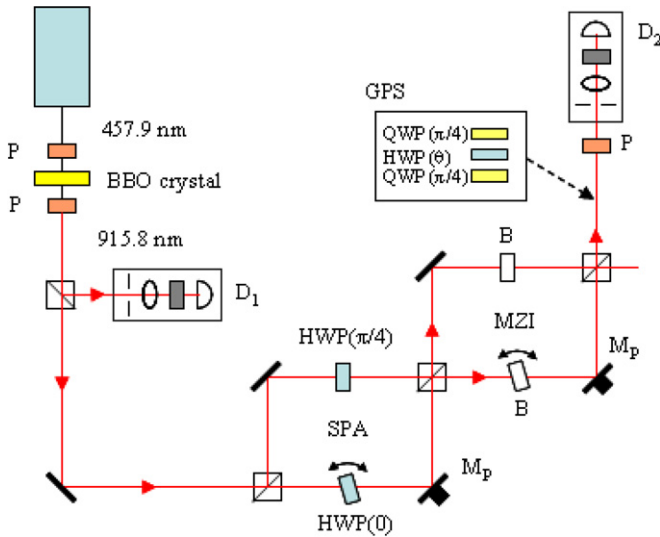


Figure 2. Experimental setup. Photon pairs produced by parametric down-conversion with a BBO crystal. We used Glan–Thompson polarizers (P), half-wave plates (HWP(angle)), optical blanks (B), mirrors mounted on piezo-driven stages (M_p), and a geometric-phase shifter (GPS) to manipulate the state of the light. The GPS consisted of two quarter-wave plates with a half-wave plate in between. Detector modules (D_1, D_2) had iris, lens, band-pass filter and avalanche photodiode.

To the last two terms of equation (19), $P_Y^{\text{cl}}(\alpha')$ and $P_V^{\text{cl}}(\beta)$, it corresponds the quantum mechanical probabilities $P_Y(\alpha')$ and $P_V(\beta)$, respectively. These last ones can be transformed in the following way, for any α'' and β'' :

$$P_Y(\alpha') = P_{YV}(\alpha', \beta'') + P_{YH}(\alpha', \beta'') \quad (21)$$

$$P_Y(\alpha') = P_{YV}(\alpha', \beta'') + P_{YV}(\alpha', \beta'' + \pi/2) \quad (22)$$

and

$$P_V(\beta) = P_{YV}(\alpha'', \beta) + P_{XV}(\alpha'', \beta) \quad (23)$$

$$P_V(\beta) = P_{YV}(\alpha'', \beta) + P_{YV}(\alpha'' + \pi/2, \beta). \quad (24)$$

Under these operations then $S_{\text{CH}} = S_{\text{CH}}(\alpha, \alpha', \alpha'', \beta, \beta', \beta'')$. If we pick, for example, $\alpha'' = \alpha$ and $\beta'' = \beta$ we get

$$S_{\text{CH}} = -P_{YV}(\alpha, \beta') + P_{YV}(\alpha', \beta') - P_{YV}(\alpha', \beta'_\perp) - P_{YV}(\alpha_\perp, \beta), \quad (25)$$

where we use the notation $\alpha_\perp = \alpha + \pi/2$. When $\alpha = -\pi/4, \alpha' = -\pi/2, \beta = -3\pi/8$ and $\beta' = 3\pi/8$ we get $S_{\text{CH}} = 0.207$, which is a violation of (19). We note that the form of equation (25) depends on the choice of α'' and β'' in equations (22) and (24), α and β , respectively. Other forms can be obtained, although they all give the same result for a given value of angles.

However, inequality (19) was derived without explicitly assuming that classical probabilities satisfy relations such as equations (22) and (24), which hold for quantum mechanical probabilities. Hence, we would not have a valid test of the CH inequality, unless we prove that equations analogous to equations (22) and (24) do hold true for classical probabilities. We argue they do, though we should remark that the class

of hidden-variable models that our test rules out must be accurately defined. We deal with this matter below.

Let us denote by $p_Y(\lambda, \alpha)$ the classical probability for a photon to follow the Y branch of our apparatus, when the first MZI was set to α , whereby the hidden variables happened to take the particular value λ when the photon was emitted. Similarly, $p_V(\lambda, \beta)$ means the classical probability for a photon to have the polarization β when the hidden variables took the value λ . Let us now set $x = p_Y(\lambda, \alpha), x' = p_Y(\lambda, \alpha + \pi/2), y = p_V(\lambda, \beta), y' = p_V(\lambda, \beta + \pi/2)$. Replacing these values in the inequality $xy - xy' + x'y + x'y' - x' - y \leq 0$, multiplying the result by $\rho(\lambda)$ and integrating it over λ , we obtain

$$P_{YV}^{\text{cl}}(\alpha, \beta) - P_{YV}^{\text{cl}}(\alpha, \beta + \pi/2) + P_{YV}^{\text{cl}}(\alpha + \pi/2, \beta) + P_{YV}^{\text{cl}}(\alpha + \pi/2, \beta + \pi/2) - P_Y^{\text{cl}}(\alpha + \pi/2) - P_V^{\text{cl}}(\beta) \leq 0. \quad (26)$$

Here, $P_{YV}^{\text{cl}}(\alpha, \beta) = \int d\lambda \rho(\lambda) p_Y(\lambda, \alpha) p_V(\lambda, \beta), P_Y^{\text{cl}}(\alpha) = \int d\lambda \rho(\lambda) p_Y(\lambda, \alpha), P_V^{\text{cl}}(\beta) = \int d\lambda \rho(\lambda) p_V(\lambda, \beta)$. This is the inequality we have tested and shown that is experimentally violated, in accordance with the quantum-mechanical predictions.

We relate S_{CH} to the measurements in the following way. The measured probabilities are

$$P_{YV}(\alpha, \beta) = \frac{N_{YV}(\alpha, \beta)}{\eta N}, \quad (27)$$

where $N_{YV}(\alpha, \beta)$ are the measured detections in a time t_0 , η is the detection efficiency and N the number of down-converted pairs in the time t_0 . Since η is the same for all measurements we can define $S'_{\text{CH}} \equiv S_{\text{CH}}\eta N/2$, which translates into the inequality

$$S'_{\text{CH}} = -N(\alpha, \beta') + N(\alpha', \beta') - N(\alpha', \beta'_\perp) - N(\alpha_\perp, \beta) \leq 0. \quad (28)$$

Thus, since the inequality is compared to zero *all the efficiencies cancel out*. Such a reduction is generally not possible with two separate particles because they involve separate detectors, with joint probabilities containing the product of efficiencies but singles probabilities containing only singles efficiencies. In such cases the cancellation of efficiencies is not complete. For a product of efficiencies to appear in connection to singles probabilities these should be expressible in terms of joint probabilities, similarly to equations (21) and (23). We are not aware of two-particle experiments in which this condition makes sense. However, Clauser and Horne (1974) proposed a way to achieve a cancellation of efficiencies in the two-photon case and some experiments were in fact performed along these lines, based on two-photon correlations (Ou and Mandel 1988, Torgerson *et al* 1995). Now, in the two-photon experiments performed by Ou and Mandel the singles probabilities could be replaced by joint probabilities only under a supplementary assumption, namely the ‘no-enhancement assumption’ (Clauser and Horne 1974, Ou and Mandel 1988). Under this supposition singles probabilities are bounded by probabilities corresponding to measurements in which a change in the experimental arrangement has been undertaken (a polarizer has been

removed). Though this is a reasonable assumption, it further restricts the class of hidden-variable models under test, because by dropping this additional assumption it becomes possible to construct realistic models that mimic quantum mechanics (Clauser and Horne 1974). In our case, we do not need to invoke the ‘no-enhancement assumption’ for equations (21) and (23) to hold true, and hence our experiments test a broader class of non-contextual realistic models, than previous ones. This includes the experiments of Torgerson *et al* (1995). Indeed, although these authors do not invoke the no-enhancement assumption, they do assume that singles probabilities satisfy, e.g., $P_1(\theta_1) = P_{12}(\theta_1, \theta_2) + P_{12}(\theta_1, \theta_2 + \pi/2)$, i.e., a condition similar to our equations (22) and (24), but with P_1 referring to measurements at one detector and P_{12} referring to joint measurements at two different detectors.

In contrast to our case, where only a single detector is involved, in the two-particle case—with two detectors involved—the above condition cannot be generally satisfied. This is because its left-hand side refers to a singles probability (whose value depends on the efficiency of one detector) whereas its right-hand side entails joint probabilities (whose values depend on two independent efficiencies). Excepting the case of ideal detectors, the above condition would not be generally satisfied, independently of the fair sampling assumption that Torgerson *et al* invoke to justify it. In our case, the validity of equations (21) and (23) can be safely stated, though, as already said, we should take care to properly delimit the class of models that we are putting to the test. In what follows, we discuss the class of HV models that our test rules out.

First, we have assumed that, for example, $p_{YV}(\lambda, \alpha, \beta) = p_Y(\lambda, \alpha)p_V(\lambda, \beta)$. This means that the probability for a photon to follow the Y -branch is for all angles α and β independent of its polarization state. In a standard test with polarizers on polarization-correlated photon pairs the corresponding assumption is a natural one, because a probability like $p_{YV}(\lambda, \alpha, \beta)$ refers to two distant measurements on two different particles, and locality can thus be invoked. In our case, locality is not an issue and the above assumption is based on non-contextuality, which here amounts to an independence assumption between the two photon’s degrees of freedom we are dealing with, i.e., momentum and polarization. On the other hand, our particular way of measuring the individual probabilities (see equations (22) and (24)) presupposes that, at the classical level, $\int p_Y(\lambda, \alpha)\rho(\lambda) d\lambda = \int p_Y(\lambda, \alpha)[p_V(\lambda, \beta) + p_V(\lambda, \beta + \pi/2)]\rho(\lambda) d\lambda$ for all β . This follows from the assumption that $p_V(\lambda) = p_V(\lambda, \beta) + p_V(\lambda, \beta + \pi/2) = 1$, which states that the probability of detecting a photon equals the sum of two probabilities, namely the probability of detecting it when the polarizer is set to an arbitrary angle β , plus the probability of detecting it when the polarizer is set perpendicularly to the first orientation, i.e. to an angle $\beta + \pi/2$. While it is an experimental fact that this relation is true—commonly expressed through Malus’ law—it should be stated explicitly to properly delimit the class of HV models being tested. Similar assumptions are made with respect to the other individual probability, namely $P_V(\beta) = P_{YV}(\alpha, \beta) + P_{YV}(\alpha + \pi/2, \beta)$, which follows from

$p_Y(\lambda) = p_Y(\lambda, \alpha) + p_Y(\lambda, \alpha + \pi/2) = 1$. This last equality is in accordance with the fact that when $\Delta\phi = 2\alpha$ is changed by π the outputs of the two ports of the MZI are interchanged. Obviously, the photon must exit the MZI by one or the other port.

3. Experimental procedure

We carried out the experiments with heralded photons entangled in spatial and polarization modes with the general scheme presented in the previous section, but with some differences noted below. Collinear photon pairs at a wavelength of 915.8 nm were produced by type-I spontaneous parametric down conversion of 457.9 nm light from a continuous-wave argon-ion laser operating at about 200 mW. The pairs were split by a nonpolarizing beam splitter, as shown in the apparatus schematic of figure 2. The photons coming off the reflection port of the beam splitter were sent directly to a bare avalanche photodiode single-photon detector (D_1 in figure 2) preceded by an iris, a lens and a 10 nm band-pass filter. The detector had a 30% efficiency at the wavelength of the down-converted photons.

The polarization of the pump light was set to be horizontal. A Glan Thompson polarizer ensured the purity of the polarization. After the down-conversion crystal, a 7 mm long beta-barium-borate crystal, the pump beam and any stray light from the laser was extinguished by a Glan-Thompson polarizer set to the vertical direction. As such, only the vertically-polarized down-converted photons and a very attenuated fraction of the pump beam passed through the polarizer. The remaining pump light was blocked by the band-pass filters in front of the detectors.

The SPA shown in figure 2 had identical zero-order half-wave plates in each arm. In the top arm, the optic axis of the wave-plate (HWP($\pi/4$)) was set to $\pi/4$ relative to the vertical so that the polarization of the light passing through it was flipped to the horizontal direction. The wave plate in the other arm (HWP(0)) served a dual role. With its axis oriented vertically, it left the input polarization state unchanged and served to equalize the two optical paths. In some experiments the rotation of HWP(0) about the vertical axis served to adjust the phase δ in equation (7). The two mirrors of the interferometer were mounted on translation stages for added flexibility. The optical paths were equalized via measurements of the interference produced by white light. (This challenging part of the experiments was necessary due to the short coherence length of the down-converted light determined by the detector filters.) A piezo-electric element served as a spacer in one of the stages for adjusting and scanning δ . The MZI that followed, which acted as a spatial basis rotator, was constructed in a similar fashion, with pairs of identical mirrors on stages at its corners and non-polarizing beam splitters at the input and output.

Since $\alpha = \Delta\phi/2$ is a critical parameter of these measurements, we performed experiments that differed in the way in which $\Delta\phi$ was varied. In one set of measurements, labelled here as setup ‘I’, the phases δ and α were set by adjusting the piezo-electric spacers on the stages where

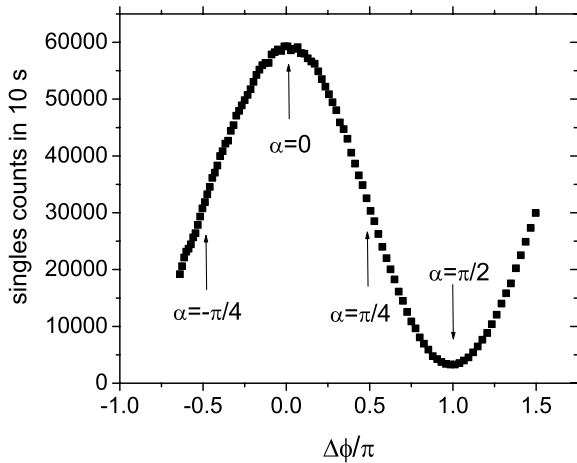


Figure 3. Example of an experimental run used to obtain the value of $\alpha = \Delta\phi/2$. For the data shown in the figure we varied $\Delta\phi$ by changing the length of one of the arms of the MZI. This was done by scanning the voltage of a piezo-electric spacer in a stage where one of the mirrors of the interferometer was mounted.

the corresponding mirrors were mounted (M_P in figure 2). A voltage applied to the piezo-electric elements moved the corresponding mirrors.

In experiments with the setup labelled ‘II’ the values of $\Delta\phi$ were set by the tilt of a 5 mm optical blank in one of the arms of the MZI (see figure 2). The optical element was mounted on a motorized rotation stage. In the other arm, a fixed identical blank was used to compensate the path lengths of the two arms. In these experiments δ was also set by tilting HWP(0), as mentioned earlier. The voltage of the piezo-electric spacers was kept at zero.

The values of α were determined by calibration runs done before every measurement. An example of a calibration run is shown in figure 3.

The calibration for α was done by blocking the x input of MZI and by scanning the voltage on the piezo-electric, or the tilt of the rotating optical flat. We determined the settings $\alpha = 0$, $\alpha = \pm\pi/4$ and $\alpha = \pi/2$ by locating the angles where we got the maximum, half-maximum and minimum counts in the interference output, respectively. We did these calibrations with the singles counts, which were typically 70 000 at maxima and 4000 at minima. We did so on the singles because these were in phase with the coincidence counts and typically a factor of a 100 larger in value. We did fits to the data and determined the uncertainty in alpha to be 2° .

Recording the measurements of each of the ports of the apparatus can give us the probabilities that we need for calculating S . However, more practical is to measure a single set of projections and appeal to the fair sampling assumption. This can be done because all of the projections of equations (12)–(15) can be obtained with a single detector via the following relations: $P_{YH}(\alpha, \beta) = P_{YV}(\alpha, \beta - \pi/2)$, $P_{XV}(\alpha, \beta) = P_{YV}(\alpha - \pi/2, \beta)$, $P_{XH}(\alpha, \beta) = P_{YV}(\alpha - \pi/2, \beta - \pi/2)$. We could exploit this fact and still obtain a valid test of realistic non-contextual HV theories, as was explained before. By using one detector we also avoided the problem of detectors with different efficiencies.

The use of one detector allowed us to directly project the state of polarization of the light into a rotated basis using a rotating polarizer. Past the y output port of the MZI we had a Glan–Thompson polarizer followed by a detector arrangement (D_2 in figure 2) similar to that used for detecting the heralding photons. The value of β was obtained by the angular position of the Glan–Thompson polarizer, which had an uncertainty of 0.5° .

There was an additional technical problem that arose. As mentioned earlier, the y output port of the MZI was chosen for making the spatial projection of the light. The vertically polarized light entered and excited the interferometer through the y ports. However, horizontally polarized light entered through the x input port and excited through the y output port. We found that non-ideal reflection phases inserted a phase between the horizontal and vertical components of the light leaving the MZI.

In one version of our setup we placed a geometric-phase shifter after the MZI, as shown in figure 2. The phase shifter consisted of two quarter-wave plates oriented at the same angle of $\pi/4$ with respect to the horizontal, with a half-wave plate in between. By setting the half-wave plate to an angle θ , the three-element device inserted a Pancharatnam–Berry geometric phase of 4θ between the horizontal and vertical components of the light input to it (Martinelli and Vavassori 1990). This adjustment allowed us to cancel the non-ideal reflection phases of the interferometer by finding the geometric phase that yielded the highest visibility when the polarizer setting was $\beta = \pi/4$. In other experiments we removed the phase shifter and instead adjusted the value of δ to compensate for the nonideal phases.

4. Results

4.1. Clauser–Horne–Shimony–Holt violation

We made several measurements of spatial-polarization correlations leading to a value of the S_{CHSH} correlation parameter of the CHSH inequality. We considered the following settings of the spatial and polarization projections that lead to a violation of the CHSH inequality for normalized correlation functions: $\alpha = -\pi/4$, $\alpha' = -\pi/2$, $\beta = -3\pi/8$ and $\beta' = 3\pi/8$.

The values of α were set differently in setups I and II, as mentioned earlier. The values of the correlation parameter S_{CHSH} for measurements using setups I and II were 2.77 ± 0.06 and 2.47 ± 0.06 , respectively. Both cases I and II violate the inequality by 12 and 7 standard deviations, respectively. Figure 4 shows data (symbols) on the correlations that led to the violation using setup II. The solid line is a fit of the data taken with $A\{1 + V \cos[(\alpha - \beta)/2]\}$, where the amplitude A and the visibility V were the fitted parameters. The latter was $V = 0.89 \pm 0.03$. If we were to use the fitted values we would get $S_{\text{CHSH}} = 2.51 \pm 0.06$.

In an effort to test our procedures we did a measurement of the S parameter of the CHSH inequality for a case where the inequality is *not* violated. By considering the angles $\alpha = -\pi/3$, $\alpha' = -\pi/6$, $\beta = 0$ and $\beta' = \pi/4$ the quantum-mechanical prediction is $S_{\text{CHSH}} = 0$. A measurement using

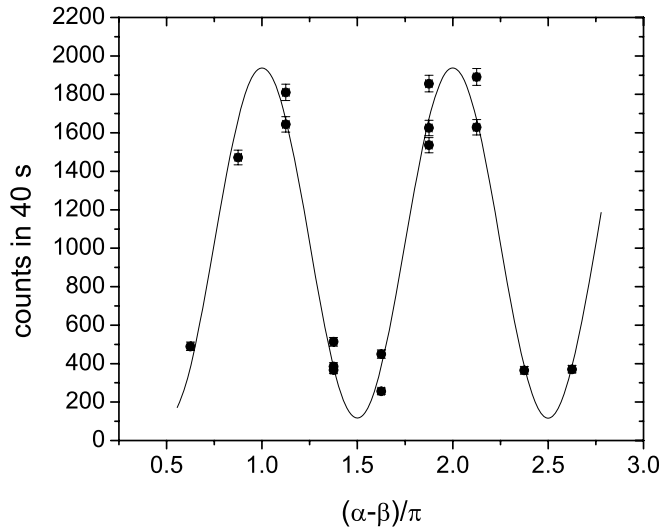


Figure 4. Data (symbols) obtained with setup II that was used to compute the correlation parameter S_{CHSH} that violated the CHSH inequality. The solid line is a single parameter fit to the data.

Table 1. Measured values of S'_{CH} for different values of α'' and β'' in equations (22) and (24).

α''	β''	S'_{CH}
α	β	1343 ± 63
α	β'	1181 ± 61
α'	β	1543 ± 93
α'	β'	1381 ± 61

setup II gave $S_{\text{CHSH}} = -0.19 \pm 0.07$, which is consistent with the expectation that for these values of the angles the inequality was satisfied. A fit to the data similar to that of figure 4 gave $V = 0.78 \pm 0.02$; we also got $S_{\text{CHSH}} = 0 \pm 0.07$ with the fitted values.

4.2. Clauser–Horne inequality violation

We tested the CH inequality with our data as described earlier. The form of the CH inequality in equation (25) was obtained by using $\alpha'' = \alpha$ and $\beta'' = \beta$ in equations (22) and (24). Our result using this form of the CH inequality (equation (28)) is listed in the first row of table 1. These measurements used setup I for the case $\alpha = -\pi/4$, $\alpha' = -\pi/2$, $\beta = -3\pi/8$ and $\beta' = 3\pi/8$. We got results for other equivalent forms of S_{CH} obtained by using different choices of α'' and β'' listed in the other rows of table 1. The weighted average of the measurements is 1333 ± 21 , where the uncertainty is the standard deviation of the mean. This is a violation of the CH inequality by more than 63 standard deviations. We note that the same apparatus and signals give us a greater violation with the CH inequality than with the CHSH inequality.

Finally, given that we perform consecutive measurements at different angles, and given that we do not have perfect efficiencies, we have to appeal to the fair sampling assumption, i.e., that our measurements are representative of what would have been obtained with simultaneous detections and perfect efficiencies.

5. Conclusions

In summary, we have presented two violations of CHSH and CH inequalities with single photons bearing two qubits. These violations rule out a broad class of realistic non-contextual HV theories in favor of quantum mechanics. We performed the tests of the CHSH and the CH inequalities with one and the same setup. The test of the CH inequality is new and provides a more stringent test than that of the CHSH inequality. It removes some of the objections that have been raised to the large group of CHSH inequality violations with normalized correlation parameters (Santos 2004).

It is interesting to note that by enabling another degree of freedom to the photon, e.g., by using the spatial modes of the light, which carry orbital angular momentum, we could perform the all-or-nothing Greenberger–Horne–Zeilinger test (Greenberger *et al* 1989) with a single particle. This would open new doors to tests of non-contextual HV theories with single particles.

Acknowledgments

We wish to acknowledge useful discussions with V Mansfield. This work was funded by grant DUE-0442882 from the National Science Foundation and Colgate University.

References

- Aspect A 2007 *Nature* **446** 866–7
- Aspect A, Dalibard J and Roger G 1982 *Phys. Rev. Lett.* **49** 1804–7
- Aspect A, Grangier P and Roger G 1981 *Phys. Rev. Lett.* **47** 460–3
- Aspect A, Grangier P and Roger G 1982 *Phys. Rev. Lett.* **49** 91–4
- Barreiro J, Lankford N K, Peters N A and Kwiat P G 2005 *Phys. Rev. Lett.* **95** 260501
- Bell J S 1965 *Physics* **1** 195–200
- Bell J S 1966 *Rev. Mod. Phys.* **38** 447–52
- Bouwmeester D, Pan J-W, Daniell M, Weinfurter H and Zeilinger A 1999 *Phys. Rev. Lett.* **82** 1345–8
- Cabello A and Larsson J-A 2007 *Phys. Rev. Lett.* **98** 220402
- Clauser J F and Horne M A 1974 *Phys. Rev. D* **10** 526–35
- Clauser J F, Horne M A, Shimony A and Holt R A 1969 *Phys. Rev. Lett.* **23** 777–80
- Clauser J F and Shimony A 1978 *Found. Phys.* **41** 1881–927
- De Zela F 2007 *Phys. Rev. A* **76** 042119
- Eberhard P H 1993 *Phys. Rev. A* **47** R747
- Einstein A, Podolsky P and Rosen N 1935 *Phys. Rev.* **47** 777
- Englert B-G, Kurtsiefer C and Weinfurter H 2001 *Phys. Rev. A* **63** 032303
- Garg A and Mermin N D 1987 *Phys. Rev. D* **35** 3831
- Greenberger D M, Horne M A and Zeilinger A 1989 *Bell's Theorem, Quantum Theory, and Conceptions of the Universe* ed M Kafatos (Dordrecht: Kluwer) p 73
- Greenberger D M, Horne M A and Zeilinger A 1995 *Phys. Rev. Lett.* **75** 2064
- Groblacher S, Paterek, Kaltenbaek R, Brukner C, Zukowski M, Aspelmeyer M and Zeilinger A 2007 *Nature* **446** 871–5
- Hardy L 1994 *Phys. Rev. Lett.* **73** 2279
- Hasegawa Y, Loidl R, Badurek G, Baron M and Rauch H 2003 *Nature* **425** 45–8
- Huang Y F, Li C F, Zhang Y S, Pan J W and Guo G C 2003 *Phys. Rev. Lett.* **90** 250401
- Kochen S and Specker E 1967 *J. Math. Mech.* **17** 59–87
- Lapiedra R 2006 *Europhys. Lett.* **75** 202
- Mair A, Vaziri A, Weihs G and Zeilinger A 2001 *Nature* **412** 313–6

- Malley J D 1998 *Phys. Rev. A* **58** 812
- Martinelli M and Vavassori P 1990 *Opt. Commun.* **80** 166–76
- Michler M, Weinfurter H and Zukowski M 2000 *Phys. Rev. Lett.* **84** 5457–61
- Ou Z Y and Mandel L 1988 *Phys. Rev. Lett.* **61** 50–3
- Peres A 1995 *Phys. Rev. Lett.* **74** 4571
- Rowe M A, Kielpinski D, Meyer V, Sackett C A, Itano W M, Monroe C and Wineland D J 2001 *Nature* **409** 791–4
- Santos E 2004 *Found. Phys.* **34** 1643–73
- Tan S M, Walls D F and Collet M J 1991 *Phys. Rev. Lett.* **66** 252
- Tittel W, Brendel J, Sbinden H and Gisin N 1998 *Phys. Rev. Lett.* **81** 3563–6
- Torgerson J R, Branning D, Monken C H and Mandel L 1995 *Phys. Rev. A* **51** 4400–04
- Weihls G, Jennewein T, Simon C, Weinfurter H and Zeilinger A 1998 *Phys. Rev. Lett.* **81** 5039–43
- Wheeler J A and Zurek W H 1983 *Quantum Theory and Measurement* (Princeton, NJ: Princeton University Press)